

Scale Setting for QCD with Four Dynamical Quarks

R. Höllwieser, F. Knechtli, T. Korzec

published in

NIC Symposium 2020

M. Müller, K. Binder, A. Trautmann (Editors)

Forschungszentrum Jülich GmbH,
John von Neumann Institute for Computing (NIC),
Schriften des Forschungszentrums Jülich, NIC Series, Vol. 50,
ISBN 978-3-95806-443-0, pp. 185.
<http://hdl.handle.net/2128/24435>

© 2020 by Forschungszentrum Jülich

Permission to make digital or hard copies of portions of this work for personal or classroom use is granted provided that the copies are not made or distributed for profit or commercial advantage and that copies bear this notice and the full citation on the first page. To copy otherwise requires prior specific permission by the publisher mentioned above.

Scale Setting for QCD with Four Dynamical Quarks

Roman Höllwieser, Francesco Knechtli, and Tomasz Korzec

Department of Physics, Bergische Universität Wuppertal, Gaußstr. 20, 42119 Wuppertal, Germany
E-mail: {hoellwieser, korzec}@uni-wuppertal.de, knechtli@physik.uni-wuppertal.de

Monte-Carlo Simulations of QCD with dynamical up, down, strange and charm quarks are carried out on lattices with large volumes and fine lattice spacings using a new massive renormalisation and improvement scheme that is tailored towards situations with a dynamical charm quark. The lattice spacings of the generated ensembles are determined and first physical results, concerning the mass spectrum of mesons built from a charm and anti-charm quark, are presented.

1 Introduction

1.1 Quantum Chromodynamics

Quantum Chromodynamics (QCD) is the theory of strong interactions. The building blocks are quark fields, that come in six different flavours, each with a different mass, and gluon fields that are the force carriers of the strong interactions. Due to the strength of the interactions and the phenomenon of confinement, the approximation that works very well in the electroweak sector, perturbation theory, is only of limited use for QCD, especially at low energies. This is however the energy region where the standard model makes many easily testable predictions. The whole hadron mass spectrum including exotic states, various properties of hadrons, like the magnetic moments of proton and neutron or their charge radii, decay constants, and a plethora of other quantities can in principle be calculated in QCD from first principles. But the only method to carry these calculations out without relying on major uncontrolled approximations is by a numerical evaluation of the QCD path integral by Monte-Carlo methods.

1.2 Lattice QCD

A formulation of QCD that is particularly well suited for numerical methods, is the lattice-regularised Euclidean path integral. A four dimensional piece of space-time of size $T \times L^3$ is discretised. A hypercubic lattice with lattice-spacing a is introduced and quark fields are only defined on the sites of this lattice instead of being continuous functions of the spacetime position. In this formulation predictions are obtained from high dimensional integrals of the form

$$\langle \mathcal{O} \rangle = \int DU \frac{1}{Z} e^{-S_g[U]} \det[D_u] \det[D_d] \det[D_s] \det[D_c] \det[D_b] \det[D_t] \mathcal{O}[U] \quad (1)$$

The integration is over all gauge field configurations

$$\int DU \equiv \prod_{x_0=0}^{T/a-1} \prod_{x_1, x_2, x_3=0}^{L/a-1} \prod_{\mu=0}^3 \int dU(x, \mu) \quad (2)$$

where $U(x, \mu)$ is a $SU(3)$ matrix on the link between site $x = (x_0, x_1, x_2, x_3)$ and its neighbour in the positive μ direction, and dU is the Haar measure of $SU(3)$. This amounts to a very high dimensional (*e. g.* around 500×10^6 dimensional for ensemble B of Tab. 1), compact, integral. $S_g[U]$ is the gauge-action. There are many different possibilities to discretise the continuum Yang-Mills action, one particular being the tree-level Symanzik improved action¹

$$S_g[U] = \frac{1}{g_0^2} \left(\frac{5}{3} \sum_p \text{tr}[1 - U_p] - \frac{1}{12} \sum_r \text{tr}[1 - U_r] \right) \quad (3)$$

where g_0 is the bare gauge coupling constant, p runs over all oriented elementary squares and r over all rectangles of size 1×2 of the lattice. U_p (U_r) are ordered products of the $SU(3)$ gauge field variables around the squares (rectangles). The contributions of the sea-quarks are encoded in the fermionic determinants $\det[D_i]$. The huge ($\approx 190 \cdot 10^6 \times 190 \cdot 10^6$ for ensemble B) matrices D_i are discretised Dirac operators, and again there are many different choices. For clover improved Wilson fermions² they are given by

$$D_i[U] = D_w + m_i + \delta D_v \quad (4)$$

$$D_w = \frac{1}{2} \{ \gamma_\mu (\nabla_\mu^* + \nabla_\mu) - \nabla_\mu^* \nabla_\mu \} \quad (5)$$

$$\delta D_v \psi(x) = c_{sw} \frac{i}{4} \sigma_{\mu\nu} \hat{F}_{\mu\nu}(x) \psi(x) \quad (6)$$

Here $\gamma_0, \dots, \gamma_3$ are Dirac matrices, $\sigma_{\mu\nu} = i\gamma_\mu \gamma_\nu$, m_i is the bare mass parameter for quark flavour i and ∇_μ (∇_μ^*) are covariant forward and backward lattice derivative operators with respect to x_μ . $\hat{F}_{\mu\nu}$ is a discretised field strength tensor. See *e. g.* Ref. 3 for an exact definition of all quantities. Z is a normalisation constant, such that $\langle 1 \rangle = 1$, and finally $\mathcal{O}[U]$ is an “observable”. For every quantity that one wants to compute, an appropriate observable has to be found, *e. g.* meson masses can be extracted from the t dependence of correlation functions with

$$\mathcal{O}[U] = \sum_{\vec{x}, \vec{y}} \text{tr}[\Gamma D_i^{-1}(x_0, \vec{x}; x_0 + t, \vec{y}) \Gamma D_j^{-1}(x_0 + t, \vec{y}; x_0, \vec{x})] \quad (7)$$

Here the space-time indices of the Dirac operators are written out explicitly, $x = (x_0, \vec{x})$, and Γ are matrices like *e. g.* $\Gamma = \gamma_5 \equiv \gamma_0 \gamma_1 \gamma_2 \gamma_3$, that select a particular symmetry channel. Note, that the inverse operators are not sparse matrices anymore!

Results of lattice QCD depend on the lattice spacing a and ultimately the continuum limit $a \rightarrow 0$ has to be taken (numerically). Due to asymptotic freedom in the continuum limit the bare coupling approaches $g_0 \rightarrow 0$. L and T are usually chosen to be large enough, that one is effectively working in the infinite volume limit.

1.3 Algorithms

The factor $p[U] \equiv \frac{e^{-S_g}}{Z} \prod_i \det[D_i]$ is real, positive (for mass-degenerate u and d quarks and heavy enough remaining quarks) and normalised, which makes it a valid probability density function for the distribution of gauge field configurations. This is the perfect starting point for Monte-Carlo methods. If a sequence of gauge field configurations

$U^{(1)}, \dots, U^{(N)}$ distributed according to p can be generated, the integral in Eq. 1 can be estimated by $\langle \mathcal{O} \rangle = \frac{1}{N} \sum_i \mathcal{O}[U^{(i)}] + O(N^{-1/2})$.

The generation of these configurations proceeds according to a variant of the Hybrid Monte-Carlo (HMC) algorithm.⁴ Even-odd and Hasenbusch mass preconditioning⁵ are applied to the determinants, before the molecular dynamics equations are integrated using multi-level higher order integrators.⁶ Linear systems involving the Dirac operators are dealt with using deflated⁷ and SAP-preconditioned⁸ Krylov space solvers. All simulations are carried out using openQCD-1.6.⁹

2 Dynamical Charm Quarks

According to the Appelquist-Carazzone decoupling theorem,¹⁰ heavy quarks have only a minor influence on low energy physics. In practice this means that replacing $\det D_i$ by 1 (a.k.a. quenching the quarks) will only introduce $O(m_i^{-2})$ errors on quantities with energies $E \ll m_i$, as long as the coupling and the remaining quark masses are chosen correctly. This is almost always applied to the heaviest quarks, the bottom and the top quark. The simplified setup spares a lot of tuning efforts, and more importantly makes a multi-scale problem more manageable. The next lighter quark, charm, is a bit of an edge case, and is treated differently by different collaborations. Its impact on low energy observables is believed to be small, at around 2 permille¹¹ level. At the same time, a dynamical charm quark may introduce large lattice artifacts of order $(am_c)^2$ or even $O(am_c)$ with unimproved or partially improved Wilson fermions. Moreover the costs of the simulations are increased and the tuning of simulation parameters is substantially more difficult. Hence *e. g.* the CLS consortium opted for simulations with a three flavour action.¹² There are however applications, where a dynamical charm quark would be desirable, provided that the increased lattice artifacts can be controlled. One such application is charm physics, where the energies of the quantities of interest are not necessarily smaller than m_c . Although binding energies seem to be reproduced well by the effective theory,¹³ it is expected that quantities that depend on so-called disconnected charm quark diagrams are quite sensitive to the presence of a dynamical charm quark. Another is the determination of fundamental parameters of QCD. With a dynamical charm quark one has direct access to the four flavour Λ -parameter, without relying on perturbation theory.

Unimproved Wilson fermions have leading lattice artifacts of $O(a)$. This can be brought down to $O(a^2)$ by implementing the Symanzik improvement programme.¹⁴ The action is augmented by an improvement term² that, when its coefficient, c_{sw} in Eq. 6, is tuned correctly, cancels most of the $O(a)$ artifacts. In mass-independent renormalisation schemes, renormalisation and improvement factors do not depend on the quark masses. To achieve full $O(a)$ improvement in such schemes often many additional improvement coefficients need to be determined, that multiply terms proportional to quark masses. Examples are given by the b , \bar{b} and d , \bar{d} coefficients in the expression for the renormalised, improved quark mass¹⁵

$$\begin{aligned} \bar{m}_i = Z_m(\tilde{g}_0^2, a\mu) & \left[m_{q,i} + (r_m(\tilde{g}_0^2) - 1) \frac{\text{tr}[M_q]}{N_f} + a \left\{ b_m(g_0^2) m_{q,i}^2 + \bar{b}_m(g_0^2) \text{tr}[M_q] m_{q,i} \right. \right. \\ & \left. \left. + (r_m(g_0^2) d_m(g_0^2) - b_m(g_0^2)) \frac{\text{tr}[M_q^2]}{N_f} + (r_m(g_0^2) \bar{d}_m(g_0^2) - \bar{b}_m(g_0^2)) \frac{(\text{tr}[M_q])^2}{N_f} \right\} \right] \quad (8) \end{aligned}$$

In the past these coefficients were determined approximately in perturbation theory. This could be justified by the smallness of the quark masses. With dynamical charm quarks a non-perturbative determination of these coefficients is called for.¹⁶ Alternatively – and this is what we are exploring in this project – one can depart from massless schemes, and define mass-dependent renormalisation and improvement factors, resulting in a largely simplified $O(a)$ improvement pattern.

$$\bar{m}_i = \tilde{Z}_m(g_0^2, a\mu, aM) [m_i - \tilde{m}_{\text{crit}}(g_0^2, \text{atr}[M_q])] \quad (9)$$

The clover coefficient c_{sw} for a physical value of the charm quark mass and degenerate light quark masses corresponding to their average in nature was determined in Ref. 17 to a high accuracy, and here we use this action for the first time in large volume simulations.

3 Scale Setting

The lattice spacing a is not a parameter of the simulation. What can be adjusted, are the dimensionless bare coupling g_0 and the bare quark masses in lattice units am_u, am_d, am_s, am_c , non of which have a physical meaning. The results of a simulation are then (physical) quantities expressed in multiples of the unknown lattice spacing, *e. g.* the masses of pions am_π , kaons am_K , D -mesons am_D and all other hadron masses, or their decay constants af_π *etc.* In principle the mass parameters can be tuned such that a set of ratios of meson masses takes their physical values. One last quantity, *e. g.* f_π can then be used to determine the lattice spacing, *i. e.* to “set the scale”, $a = af_\pi / f_\pi^{\text{experimental}}$. Simulations at physical masses are extremely expensive and feasible only at rather coarse lattice spacings, if at all. The scale setting therefore is complicated by chiral extrapolations in the light quark masses. For high precision also electro-magnetic effects need to be taken into account. Fortunately some quantities are known to a high precision also at non-physical quark masses, from earlier simulation projects, which can be used to greatly simplify the scale setting procedure. One such quantity is the gradient flow scale t_0 ¹⁸ at a mass point where $\bar{m}_u = \bar{m}_d = \bar{m}_s$ and $12m_\pi^2 t_0 = 1.11$.

$$\sqrt{8t_0^*} = 0.413(5)(2) \text{ fm} \quad (10)$$

To set the scale with a new action, one only needs to carry out simulations at this unphysical mass point (denoted by the \star symbol), and to determine t_0^*/a^2 .

4 Simulations and Results

The goal is to find simulation parameters that correspond to quark masses implicitly given by $m_u = m_d = m_s$ and

$$\phi_4 \equiv 8t_0 \left(m_K^2 + \frac{m_\pi^2}{2} \right) = 1.11 \quad (11)$$

$$\phi_5 \equiv \sqrt{8t_0} (m_{D_s} + 2m_D) = 11.94 \quad (12)$$

and lattice spacings $a \in \{0.054, 0.041, 0.032\}$ fm. The QCD formulation is a tree-level Symanzik improved gauge action paired with non-perturbatively $O(a)$ improved Wilson fermions, in a massive scheme.¹⁷ Once the correct simulation parameters are found, high

ens.	$\frac{T}{a} \times \frac{L^3}{a^3}$	$6/g_0^2$	$am_{u,d,s}$	am_c	$a[\text{fm}]$	Lm_π^*	N_{traj} (MDUs)
A0	96×16^3	3.24	-0.27996	-0.088861	0.054	1.75	1000 (2000)
A1	96×32^3	3.24	-0.27996	-0.088861	0.054	3.5	3908 (7816)
A2	128×48^3	3.24	-0.27996	-0.088861	0.054	5.3	3868 (7736)
B	144×48^3	3.43	-0.32326	-0.17971	0.041	4.4	3030 (6060)
C	192×64^3	-	-	-	0.032	-	0 (0)

Table 1. Summary of finished and planned ensembles.

ens.	N_{ms}	t_0/a^2	$am_{\pi,K}$	am_{D,D_s}	ϕ_4	ϕ_5
A0	500	8.83(23)	0.310(6)	0.614(17)	10.22(90)	15.48(43)
A1	1954	7.43(4)	0.1137(8)	0.5247(7)	1.159(17)	12.168(40)
A2	1934	7.36(3)	0.1107(3)	0.5228(4)	1.087(6)	12.059(20)
B	1515	11.55(6)	0.0910(4)	0.4183(7)	1.148(12)	12.0627(32)

Table 2. Tuning results for the Ensembles available so far.

statistics ensembles are generated and (among other things) t_0^*/a^2 is measured. Tab. 1 summarises the finished and planned ensembles.

Ensembles A0, A1 and A2 have the same lattice spacing and serve as a check of finite volume effects. The result is, that these are negligible for our purposes, as long as $m_\pi L > 4$, see Fig. 1.

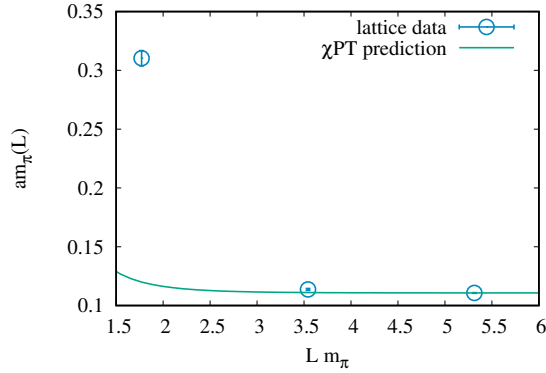


Figure 1. Finite volume effects on the pion mass, from Ensembles A0, A1 and A2.

Although we have not gathered the full statistics of ensemble *B* yet, we already roughly know the lattice spacing and can judge, how well the novel action copes with lattice artifacts. In Fig. 2 a quantity is plotted, that is supposed to vanish in the continuum limit. The rate at which it does so, is compatible with leading scaling violations of $O(a^2)$, which is very encouraging, given that these are the two coarsest ensembles that we consider.

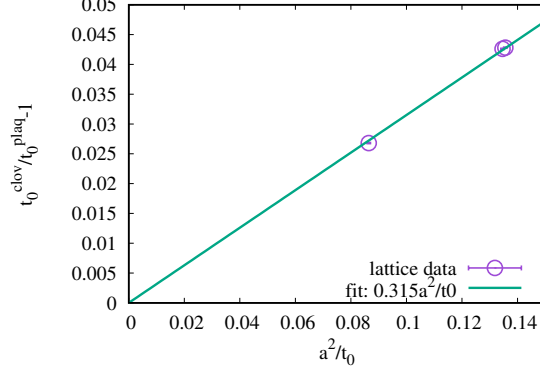


Figure 2. The relative difference of two different definitions of the gradient flow scale t_0 , which should vanish in the continuum limit at a rate proportional to a^2 .

5 Future Applications

5.1 Charmonium Spectrum

Although the ensembles generated so far are all at a non-physical mass point, the chiral extrapolations are expected to be very flat for quantities that do not contain light (u, d, s) valence quarks. The reason for this is, that the sum of the (renormalised) light quark masses has already the physical value. Therefore the sum of the differences to the physical masses is zero ($\Delta_u + \Delta_d + \Delta_s = 0$). The derivatives of these quantities with respect to the light quark masses are equal to each other at the mass-symmetric point, so in the expression for the correction between symmetrical and physical mass point, the leading term vanishes, *e. g.* for the mass of the η_c meson

$$m_{\eta_c}^{\text{phys}} = m_{\eta_c} + (\Delta_u + \Delta_d + \Delta_s) \frac{dm_{\eta_c}}{dm_u} + O(\Delta^2) \quad (13)$$

With the fine lattice spacings, our ensembles are very well suited for a study of charmonia and in fact, already at the coarsest lattice, the charmonia masses that we obtain, are very close to their values in nature. One should however note, that we are neglecting disconnected contributions to these masses at the moment. Tab. 3 summarises the findings for ensemble A2.

	η_c	J/ψ	χ_{c0}	χ_{c1}	h_c
am	0.8180(2)	0.8489(2)	0.9398(86)	0.9833(72)	0.9902(81)
m [GeV]	2.9890(7)	3.1019(7)	3.434(31)	3.593(26)	3.618(30)
PDG [GeV]	2.9834(5)	3.096900(6)	3.4148(3)	3.51066(7)	3.52538(11)

Table 3. Masses of charmonium states on ensemble A2 together with their PDG¹⁹ values.

5.2 Strong Coupling

In determinations of the strong coupling constant as done by the ALPHA collaboration, an intermediate result is the Λ -parameter in multiples of a simulated box size L . The L/a values of the finite volume simulations that enter this determination are of course known, but to obtain the physical value of Λ , the lattice spacings need to be known, too. For the planned case of four flavours they are provided by this project.

5.3 Chiral Trajectories

If, at some point, $N_f = 2 + 1 + 1$ simulations of QCD with improved Wilson quarks are desired, this work provides a formidable starting point. The quantities ϕ_4 and ϕ_5 are chosen such, that \overline{m}_c and $\overline{m}_u + \overline{m}_d + \overline{m}_s$ have nearly their physical values. The physical mass point can be approached along chiral trajectories where $\overline{m}_u = \overline{m}_d$ is decreased and \overline{m}_s is increased, while the trace of the quark mass matrix is kept constant. This is a strategy which is particularly well suited for Wilson fermions, and which has been already successfully employed in Ref. 12, 20. No expensive tuning of simulation parameters is required anymore.

6 Conclusions

First Monte-Carlo simulations of QCD with a novel action that is tailored towards simulations including a dynamical charm quark have been carried out on the mass-symmetrical points of relatively fine lattices. The lattice artifacts seem to be relatively mild and more importantly in agreement with $O(a^2)$ scaling, already at the coarsest ensemble. The scale has been set and the ground state masses of a few charmonia have been computed. Already at the coarsest lattice a reasonable agreement with their values in nature is found. All of this encourages us to carry on with the last ensemble with finest lattice spacing.

Acknowledgements

We gratefully acknowledge the Gauss Centre for Supercomputing (GCS) for providing computer time at the supercomputer JUWELS at the Jülich Supercomputing Centre (JSC) under GCS/NIC project ID HWU35. R. H. was supported by the Deutsche Forschungsgemeinschaft in the SFB/TR55.

References

1. M. Lüscher and P. Weisz, *On-Shell Improved Lattice Gauge Theories*, Commun. Math. Phys. **97**, 59, 1985, [Erratum: Commun. Math. Phys. **98**, 433, 1985].
2. B. Sheikholeslami and R. Wohlert, *Improved Continuum Limit Lattice Action for QCD with Wilson Fermions*, Nucl. Phys. B **259**, 572, 1985.
3. M. Lüscher, S. Sint, R. Sommer, and P. Weisz, *Chiral symmetry and $O(a)$ improvement in lattice QCD*, Nucl. Phys. B **478**, 365–400, 1996.

4. S. Duane, A. D. Kennedy, B. J. Pendleton, and D. Roweth, *Hybrid Monte Carlo*, Phys. Lett. B **195**, 216–222, 1987.
5. M. Hasenbusch, *Speeding up the hybrid Monte Carlo algorithm for dynamical fermions*, Phys. Lett. B **519**, 177–182, 2001.
6. I. P. Omelyan, I. M. Mryglod, and R. Folk, *Symplectic analytically integrable decomposition algorithms: classification, derivation, and application to molecular dynamics, quantum and celestial mechanics simulations*, Computer Physics Communications **151**, 272–314, 2003.
7. M. Lüscher, *Local coherence and deflation of the low quark modes in lattice QCD*, JHEP **07**, 081, 2007.
8. M. Lüscher, *Solution of the Dirac equation in lattice QCD using a domain decomposition method*, Comput. Phys. Commun. **156**, 209–220, 2004.
9. M. Lüscher and S. Schaefer, *Lattice QCD with open boundary conditions and twisted-mass reweighting*, Comput. Phys. Commun. **184**, 519–528, 2013.
10. T. Appelquist and J. Carazzone, *Infrared Singularities and Massive Fields*, Phys. Rev. D **11**, 2856, 1975.
11. F. Knechtli, T. Korzec, B. Leder, and G. Moir, *Power corrections from decoupling of the charm quark*, Phys. Lett. B **774**, 649–655, 2017.
12. M. Bruno *et al.*, *Simulation of QCD with $N_f = 2 + 1$ flavors of non-perturbatively improved Wilson fermions*, JHEP **02**, 043, 2015.
13. S. Cali, F. Knechtli, and T. Korzec, *How much do charm sea quarks affect the charmonium spectrum?*, Eur. Phys. J. C **79**, 607, 2019.
14. K. Symanzik, *Continuum Limit and Improved Action in Lattice Theories: I. Principles and ϕ^4 Theory*, Nucl. Phys. B **226**, 187–204, 1983.
15. T. Bhattacharya, R. Gupta, W. Lee, S. R. Sharpe, and J. M. S. Wu, *Improved bilinears in lattice QCD with non-degenerate quarks*, Phys. Rev. D, **73**, 034504, 2006.
16. P. Korcyl and G. S. Bali, *Non-perturbative determination of improvement coefficients using coordinate space correlators in $N_f = 2 + 1$ lattice QCD*, Phys. Rev. D **95**, 014505, 2017.
17. P. Fritzsch, R. Sommer, F. Stollenwerk, and U. Wolff, *Symanzik Improvement with Dynamical Charm: A 3+1 Scheme for Wilson Quarks*, JHEP **06**, 025, 2018.
18. M. Bruno, T. Korzec, and S. Schaefer, *Setting the scale for the CLS 2 + 1 flavor ensembles*, Phys. Rev. D **95**, 074504, 2017.
19. M. Tanabashi *et al.*, *Review of Particle Physics*, Phys. Rev. D **98**, 030001, 2018.
20. W. Bietenholz *et al.*, *Flavour blindness and patterns of flavour symmetry breaking in lattice simulations of up, down and strange quarks*, Phys. Rev. D **84**, 054509, 2011.